

Virtual synchronous machines with fast current loop^{*}

Shivprasad Shivratri^{*} Zeev Kustanovich^{**} George Weiss^{*}
Benny Shani^{*}

^{*} School of Electrical Engineering, Tel Aviv University, Ramat Aviv
69978, Israel (e-mail: shivprasadshivratri8793@gmail.com,
gweiss@tauex.tau.ac.il, benny.shani@gmail.com)

^{**} Israel Electricity Company, North District, Israel (e-mail:
kustanz875@gmail.com)

Abstract: Virtual synchronous machines (VSM) are inverters that behave towards the power grid like synchronous generators. One popular way to realize such inverters are synchronverters, whose control algorithm has evolved over time, but both theoretical analysis and practical observations show that the output currents of a synchronverter are very sensitive to grid voltage measurement errors and processing delay, as well as imprecisions in the PWM process. To overcome this problem (of excessive sensitivity), we propose in this paper to use a different type of control to realize a VSM, that includes a fast current controller as the internal control loop of the inverter. Our simulations and experiments show that this results in a dramatic reduction of the sensitivity of the VSM to various kinds of measurement errors, noise and imprecision, and hence to the proper operation of such inverters. In particular, it leads to a large reduction of the total harmonic distortion of the grid currents.

Keywords: Virtual synchronous machine, frequency droop, voltage droop, inverter, synchronverter, current control, Park transformation, PI controller, anti-windup.

1. INTRODUCTION

Most distributed generators are connected to the utility grid via inverters that rely on various control algorithms to maintain synchronism. Mostly they offer no inertia, and behave as controlled current sources that produce fluctuating power. Numerous researchers are investigating how the control of future power grids should be controlled, offering competing control algorithms, see for instance the recent survey Tayyebi et al (2020). One of the proposed approaches is to emulate the behavior of synchronous generators, so that an inverter-based grid behaves like one based on synchronous generators (SG), see for instance Beck and Hesse (2007), Driesen and Visscher (2008), Zhong and Weiss (2009) or Arghir, Jouini and Dörfler (2018). This has many advantages, such as backward compatibility with the current grid, well known black start and fault ride-through procedures, and well tested primary and secondary frequency support algorithms.

Following Beck and Hesse (2007), inverters that behave towards the utility grid like synchronous machines are called *virtual synchronous machines* (VSM). One particular type of VSM are the *synchronverters*, introduced in Zhong and Weiss (2009). This type of inverter has attracted considerable attention, see for instance Alipoor, Miura and Ise (2013); Aouini, Marinescu, Kilani and

Elleuch (2015); Brown (2015); Cvetkovic, Boroyevich, Burgos, Li and Mattavelli (2015); Dong, Chi and Li (2016); Zhong and Hornik (2013); Zhong and Weiss (2011); Zhong, Konstantopoulos, Ren and Krstic (2018); Zhong, Nguyen, Ma and Sheng (2014). The hardware of a synchronverter is similar to that of a conventional three phase inverter (with any number of DC levels, most commonly 3), the novelty is in the control algorithm. The only hardware difference is that some fast acting energy storage (typically, capacitors) is required on the DC bus, to provide the energy pulses needed for the emulation of rotor inertia.

The paper Natarajan and Weiss (2017) has proposed five modifications to the synchronverter algorithm from Zhong and Weiss (2011), to improve its stability and performance. Of these, we mention here only the two most important ones: a substantial increase of the effective size of the filter inductors, by using virtual inductors, and the introduction of virtual capacitors in series with the inverter outputs, to eliminate DC components from the grid current. We propose here a further improvement, namely two current loops to regulate the grid current. This is needed to overcome the excessive sensitivity of synchronverters to grid voltage measurement errors due to sensor or A/D converter imperfections, and delays, as these errors can be very disturbing, causing strong distortions of the grid currents, especially when a synchronverter works at relatively low power. We show by simulations that the two extra current loops make the VSM much more robust to voltage and current sensing errors as well as to other errors. The same conclusion has been demonstrated also by hardware

^{*} This research was supported by the Ministry of Infrastructure, Energy and Water, Israel. We are grateful for the help from the SGI-Lab at the Joint Research Center of the European Commission located in Ispra, Italy.

in the loop experiments with an RTDS simulator, but due to space restrictions these experiments cannot be presented in this paper.

To understand on an intuitive level where the problem lies with the previous design, let us look at the simplified circuit diagram of a grid connected inverter in Fig. 1:

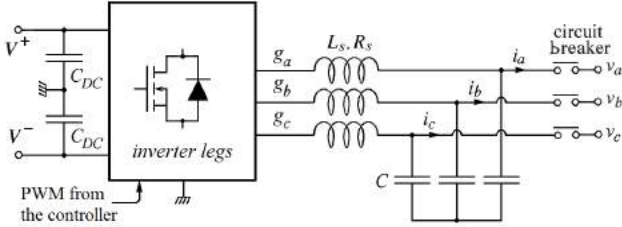


Fig. 1. An inverter with an LC filter receiving DC voltages V^+ , V^- and connected to the grid voltages v_a, v_b, v_c .

Synchronverters are voltage source converters, so that the output of the algorithm are the desired average (over one switching cycle) of the voltages g_a, g_b and g_c at the output of the inverter legs. In the original algorithm of Zhong and Weiss (2011), g_a, g_b and g_c are the internal synchronous voltages of the virtual SG, while in the version of Natarajan and Weiss (2017) they are the voltages after the virtual capacitor and the virtual inductor, as shown in Fig. 2, taken from Natarajan and Weiss (2017).

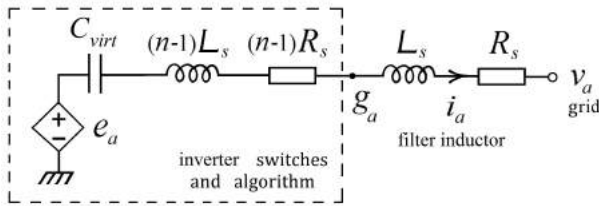


Fig. 2. A synchronverter with filter inductor L_s and its resistance R_s . e_a is the synchronous internal voltage. The inductor and resistor multiplied with $(n - 1)$ and the capacitor C_{virt} are virtual. Only phase a is shown.

A voltage measurement error Δv_a in phase a may be due to a combination of sensor imprecision, calibration errors, quantization errors, and processing delay. This error will cause a similar sized error Δg_a in the signal g_a , because g_a is closely following v_a , see formula (22) in Natarajan and Weiss (2017). This will cause an error current Δi_a that, expressed via its Laplace transform $\widehat{\Delta i}_a$, is given by:

$$\widehat{\Delta i}_a(s) = \frac{1}{L_s s + R_s} \widehat{\Delta g}_a(s).$$

For a typical inverter of 10kW nominal output, L_s would be around $2mH$, resulting in an impedance of around 0.63Ω at the nominal grid frequency of 50 Hz. Hence, having Δg_a of the order of 4V (which is a normal value according to our experience, and is a small error when expressed as a percentage of the AC voltage range) will result in Δi_a of the order of 6A, which is intolerably high. One can try to fight this phenomenon by striving for very high precision in measurements and calibrations, and devising all sorts of ingenious ways to compensate for the processing delay. However, overall this is a losing battle, and this has led us to develop an alternative solution.

Very briefly, the idea that we propose is to add current loops to the inverter, let the synchronverter work with virtual currents, which results in a very robust system, and then use the virtual currents as reference values for the current loops. This sounds simple enough, but the details are a bit tricky, especially building the current loops in such a way that they still contain the virtual capacitors, and hence will block DC components in the output current.

Synchronverters with a current loop (on the grid side) have been investigated by several researchers, see Dong, Chi and Li (2016); Mo, D'Arco and Suul (2017); Roldan-Perez, Rodriguez-Cabero and Prodanovic (2018). The paper Dong, Chi and Li (2016) also proposes how to create a multi-terminal HVDC system using synchronverters and a novel control strategy called "active voltage feedback control", providing primary and secondary frequency support. The results are supported by simulations. The other two cited references deal with smaller scale systems and they provide very good experimental results. The reasoning for using a current loop varies from author to author, but the main reason given by all is to achieve grid current limitation. In addition, Roldan-Perez, Rodriguez-Cabero and Prodanovic (2018) are also citing the reduction of current harmonics and imbalances as a reason for using current loops. Our justification (outlined above) is new, as far as we know and a more detailed analysis of the sensitivity to voltage and current sensing errors will be provided in Kustanovich et al (2020a). The main novelty in our approach is that we show how to integrate the virtual capacitors in the current loop. In addition, we give the full design of the current loops and show that they may be regarded as an internal model based controller acting at two resonant frequencies (0 and 50 Hz).

2. MODELLING THE GRID CONNECTED SYNCHRONVERTER WITH MEASUREMENT ERRORS

In this section we model the influence of the grid voltage and output current measurement errors on the synchronverter, using the models from Zhong and Weiss (2011), Natarajan and Weiss (2017), Natarajan and Weiss (2018). We follow the terminology and notation of the just cited papers. A more detailed analysis, which assesses the sensitivity of the output current with respect to the various error signal, is given in our paper Kustanovich et al (2020a). We denote by θ_g the grid angle and by ω_g the grid frequency, so that $\omega_g = \dot{\theta}_g$. This frequency ω_g is usually 100π rad/sec (corresponding to 50Hz). We denote by θ the synchronverter virtual rotor angle and its angular velocity by ω , so that $\omega = \dot{\theta}$. The difference $\delta = \theta - \theta_g$ is called the *power angle*. The notation $\widetilde{\cos\theta}$ is defined by

$$\widetilde{\cos\theta} = \left[\cos\theta \quad \cos\left(\theta - \frac{2\pi}{3}\right) \quad \cos\left(\theta + \frac{2\pi}{3}\right) \right]^T$$

and similarly

$$\widetilde{\sin\theta} = \left[\sin\theta \quad \sin\left(\theta - \frac{2\pi}{3}\right) \quad \sin\left(\theta + \frac{2\pi}{3}\right) \right]^T.$$

Then the grid voltage is

$$v = \sqrt{\frac{2}{3}} V \widetilde{\sin\theta}_g, \quad (1)$$

where V is a positive constant or a slowly changing signal.

Denote by $M_f > 0$, the peak mutual inductance between the rotor winding and any one stator winding, by i_f the variable *field current* (or rotor current) and by e the electromotive force, also called the *internal synchronous voltage*. We rewrite (4) from Zhong and Weiss (2011):

$$e = M_f i_f \omega \widetilde{\sin \theta} - M_f \frac{di_f}{dt} \widetilde{\cos \theta} \quad (2)$$

and we note that the variable current i_f governs the amplitude of e . We apply the *unitary Park transformation* $U(\theta)$ (as in Natarajan and Weiss (2018)) to (2). For any \mathbb{R}^3 -valued signal v , the first two components of $U(\theta)v$ are called the dq coordinates of v , denoted by v_d, v_q . By using the notation $m = \sqrt{3/2}M_f$, we represent the internal synchronous voltage e in dq coordinates as:

$$e_d = -m i_f \omega, \quad e_q = -m \frac{di_f}{dt}. \quad (3)$$

Often the term e_q can be neglected, because the rate of change of the field current is small, so that $e_q \ll e_d$.

Applying the Park transformation to (1), we get the dq representation of the grid voltage as

$$v_d = -V \sin \delta, \quad v_q = -V \cos \delta. \quad (4)$$

Denote by $\eta = [\eta_d \ \eta_q]^\top$ the voltage measurement errors, and by $\xi = [\xi_d \ \xi_q]^\top$ the current measurement errors, expressed in dq coordinates. This means that the synchronverter control algorithm gets $[(v_d + \eta_d) \ (v_q + \eta_q)]^\top$ as grid voltage measurements in dq coordinates. In the same way, $[(i_d + \xi_d) \ (i_q + \xi_q)]^\top$ are the measured synchronverter output currents, expressed in dq coordinates.

In our model we use the modified synchronverter equations according to Natarajan and Weiss (2017). Thus, the control algorithm computes $g = [g_a \ g_b \ g_c]^\top$ and sends it to the switches in the power part (instead of $e = [e_a \ e_b \ e_c]^\top$ in the original version of the algorithm). Writing eq. (22) from Natarajan and Weiss (2017) in dq coordinates and taking into account the measurement errors, we have

$$g_d = \frac{(n-1)(v_d + \eta_d) + e_d}{n}, \quad g_q = \frac{(n-1)(v_q + \eta_q) + e_q}{n}.$$

By applying the Park transformation on the circuit equations corresponding to Fig. 2, we have

$$L_s \frac{di_d}{dt} = -R_s i_d + \omega L_s i_q + g_d - v_d, \quad (5)$$

$$L_s \frac{di_q}{dt} = -\omega L_s i_d - R_s i_q + g_q - v_q. \quad (6)$$

Combining (3), (1) and the last three formulas, and neglecting i_q in (3) by assuming i_f to be slowly changing, we get, using the notation $R = nR_s$, $L = nL_s$,

$$L \frac{di_d}{dt} = -R i_d + \omega L i_q + V \sin \delta + (n-1)\eta_d, \quad (7)$$

$$L \frac{di_q}{dt} = -\omega L i_d - R i_q - m i_f \omega + V \cos \delta + (n-1)\eta_q. \quad (8)$$

The angular frequency evolves according to the swing equation:

$$J \frac{d\omega}{dt} = T_m - T_e - D_p \omega + D_p \omega_n, \quad (9)$$

where $J > 0$ represents the inertia of the rotor, $T_m > 0$ is the nominal active mechanical torque from the prime mover, $T_e = -m i_f (i_q + \xi_q)$ is the electric torque computed using the measured output currents and $D_p > 0$ is the

frequency droop constant. The field current i_f evolves according to eq. (15) in Natarajan and Weiss (2017):

$$M_f \frac{di_f}{dt} = \frac{1}{K} [Q_{\text{set}} - Q_{\text{est}} + D_q (v_{\text{set}} - V)], \quad (10)$$

where v_{set} is $\sqrt{2/3}$ times the desired amplitude of v , $D_q > 0$ is the voltage droop coefficient, Q_{set} is the desired reactive power, V is as in (1) and $K > 0$ is a large constant. The rms line voltage V is estimated in the algorithm as explained at the end of Section IV of Zhong and Weiss (2011), with additional strong low-pass filtering to suppress the effect of the random errors in the available voltage measurements.

The VSM output reactive power Q is $Q = v_q i_d - v_d i_q$, see for instance eq. (16) in Natarajan and Weiss (2018). An estimate of Q , denoted Q_{est} , is computed on the basis of the measured (with errors) output currents:

$$Q_{\text{est}} = V [i_q \sin \delta - i_d \cos \delta] + V [\xi_q \sin \delta - \xi_d \cos \delta]. \quad (11)$$

The following equation is a consequence of the definition of δ :

$$\frac{d\delta}{dt} = \omega - \omega_g. \quad (12)$$

The fifth order grid connected synchronverter model that includes voltage and current measurement errors can be constructed by combining the equations (7), (8), (9), (10), (11) and (12). Its state vector is $\mathbf{x} = [i_d \ i_q \ \omega \ \delta \ i_f]^\top \in \mathbb{R}^5$ and its input is the measurement error vector $\mathbf{u} = [\eta_d \ \eta_q \ \xi_d \ \xi_q]^\top \in \mathbb{R}^4$. A detailed study of this model connected to a symmetric infinite bus with frequency ω_g is in our paper Kustanovich et al (2020b), which shows that (under reasonable assumptions) this system has four equilibrium points (when δ is measured modulo 2π).

The instantaneous active power P from the synchronverter to the power grid is:

$$P = v_d i_d + v_q i_q = -V [i_d \sin \delta + i_q \cos \delta]$$

and at equilibrium, P satisfies the equation

$$[T_m + D_p (\omega_n - \omega_g)] \omega_g = P + R \frac{P^2 + Q^2}{V^2}.$$

The above formula is normally used to determine T_m if desired values for P and Q have been given.

We can compute the linearization of this model around a typical stable equilibrium point and evaluate the gains of its transfer functions from the error signals to the currents i_d and i_q at frequencies up to about 300Hz. Such a computation (see Kustanovich et al (2020a) for the details) reveals that indeed the transfer functions from voltage measurement errors to the output currents are unacceptably high, as we have argued in Section 1.

3. THE CURRENT LOOPS

We have seen that an improved synchronverter operated as in Natarajan and Weiss (2017) is very sensitive to grid voltage measurement errors, that may lead to distorted grid currents. To deal with this problem, we propose to include two current loops in a VSM, as described below. Actually, the algorithm that we describe is suitable for any inverter that receives slowly varying current reference signals in dq coordinates: $i_{d,ref}$ and $i_{q,ref}$. For a nice survey of AC current control strategies for the AC side of inverters we refer to Timbus et al (2009).

We denote by E_d and E_q be the desired output voltages at the inverter legs (before any output filter), in dq coordinates, that are computed by the current control algorithm (which will be described here). We assume that the PWM generation block and the switches work accurately, so that the averaged (over one switching period) output voltages from the inverter switches, g_a , g_b and g_c , are approximately equal to the inverse Park transformation of E_d , E_q and 0. We introduce the complex signals

$$\vec{E} = E_d + jE_q, \quad \vec{v} = v_d + jv_q, \quad \vec{i} = i_d + ji_q,$$

where $j = \sqrt{-1}$. These are time-varying phasors, as in Weiss, Dörfler and Levron (2019). Then from the equations (5) and (6) (with E_d , E_q in place of g_d , g_q) we get

$$\vec{E} - \vec{v} = R_s \vec{i} + L_s \frac{d\vec{i}}{dt} + j\omega L_s \vec{i}.$$

After applying the Laplace transformation, assuming that ω is constant and neglecting initial conditions, and denoting the Laplace transform of \vec{i} by \hat{i} , and similarly for the other signals, we get

$$\hat{i}(s) = \frac{1}{sL_s + R_s + j\omega L_s} [\hat{E}(s) - \hat{v}(s)]. \quad (13)$$

Notice that we have here a rational transfer function with non-real coefficients, a rare occurrence in control.

Denoting $z = \frac{R_s}{L_s} + j\omega_n$ and choosing a PI controller (in order to eliminate the steady-state error for constant $\vec{i}_{ref} = i_{d,ref} + ji_{q,ref}$), we get the block diagram in Fig. 3, where $\vec{\varepsilon} = \varepsilon_d + j\varepsilon_q$ is the tracking error. Note that the control algorithm adds the signal \vec{v} to the output of the PI controller, in order to cancel another signal $-\vec{v}$ entering the plant. The sensitivity S (the transfer function from the reference current \vec{i}_{ref} to $\vec{\varepsilon}$) is:

$$S(s) = \frac{s(s+z)}{s^2 + (z + \frac{K_p}{L_s})s + \frac{K_i}{L_s}}.$$

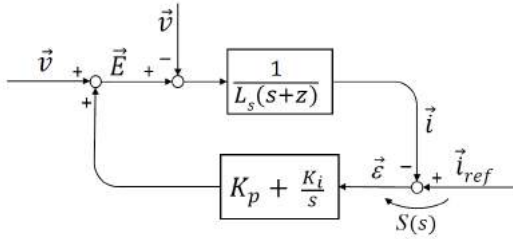


Fig. 3. Block diagram of the plant (13) with a PI controller. This is the current control loop, where the coefficients z and K_p are not real.

There are many ways to choose the controller parameters K_p , K_i , here we outline one option. We choose $K_i > 0$ and denote $\omega_b = \sqrt{K_i/L_s}$. Then we choose a complex K_p such that: $z + \frac{K_p}{L_s} = 2\omega_b$. Hence,

$$K_p = R_0 - j\omega_n L_s, \quad \text{where } R_0 = 2\omega_b L_s - R_s. \quad (14)$$

Then the transfer function from i_{ref} to i is:

$$G(s) = 1 - S(s) = \frac{(R_0/L_s - j\omega_n)s + \omega_b^2}{s^2 + 2\omega_b s + \omega_b^2}.$$

We see that bandwidth of G is approximately ω_b and there is a double pole at $-\omega_b$. If we want the current control to be fast, then we choose ω_b large, in particular, usually we choose $\omega_b > \omega_n$.

Until now, we have given the description of a general-purpose current controller. Now we make it more specific for our VSM application. Denote by $i^{virt} = [i_a^{virt} \ i_b^{virt} \ i_c^{virt}]^T$ the virtual currents computed by considering virtual impedances $R_{virt} + L_{virt}s$ connected between e and v , identically on each phase. Using such currents in the synchronverter algorithm for initial synchronization was the main idea in Zhong, Nguyen, Ma and Sheng (2014). Denote by i_d^{virt} , i_q^{virt} the dq components of i^{virt} . We set $i_{d,ref} = i_d^{virt}$ and $i_{q,ref} = i_q^{virt}$ and we apply the current control algorithm presented earlier. Thus, the tracking errors are:

$$\varepsilon_d = i_d^{virt} - i_d, \quad \varepsilon_q = i_q^{virt} - i_q. \quad (15)$$

According to Fig. 3 and (14), the components of \vec{E} are

$$\begin{aligned} E_d &= v_d + K_i \int_0^t \varepsilon_d dt + R_0 \varepsilon_d + \omega L_s \varepsilon_q, \\ E_q &= v_q + K_i \int_0^t \varepsilon_q dt + R_0 \varepsilon_q - \omega L_s \varepsilon_d. \end{aligned} \quad (16)$$

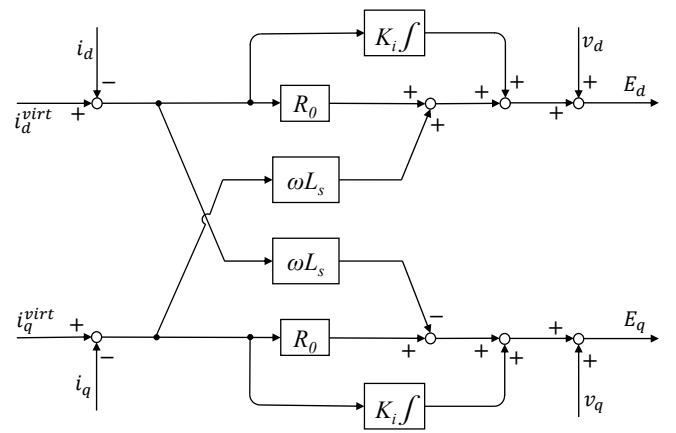


Fig. 4. The proposed current controller from (16).

Taking the inverse Park transform of $[E_d \ E_q \ 0]^T$ and putting a virtual capacitor C_{virt} in series with the output on each phase, to eliminate unwanted DC currents produced by any DC offset of the output voltages, we get:

$$\begin{aligned} g_a &= \sqrt{\frac{2}{3}} [E_d \cos \theta - E_q \sin \theta] - \frac{w_a}{C_{virt}} \\ g_b &= \sqrt{\frac{2}{3}} [E_d \cos(\theta - \frac{2\pi}{3}) - E_q \sin(\theta - \frac{2\pi}{3})] - \frac{w_b}{C_{virt}} \\ g_c &= \sqrt{\frac{2}{3}} [E_d \cos(\theta + \frac{2\pi}{3}) - E_q \sin(\theta + \frac{2\pi}{3})] - \frac{w_c}{C_{virt}}. \end{aligned}$$

Here $w = [w_a \ w_b \ w_c]^T$ are the charges in the three virtual capacitors, obtained by integrating (in the control algorithm) the measured output currents. The values g_a , g_b and g_c are sent to the inverter legs, to generate the PWM signals in the well known manner.

4. SIMULATION RESULTS

We have simulated in MATLAB/Simulink the behavior of synchronverters in a microgrid, using the older approach (the one in Natarajan and Weiss (2017)) and using the new approach presented here, under identical conditions. The simulation model in Fig. 5 is a microgrid with 3 identical inverters and 2 loads connected via transmission lines. The control part of the inverters runs in discrete time with the sampling frequency 10kHz, and the power part is simulated at a step size corresponding to 100kHz.

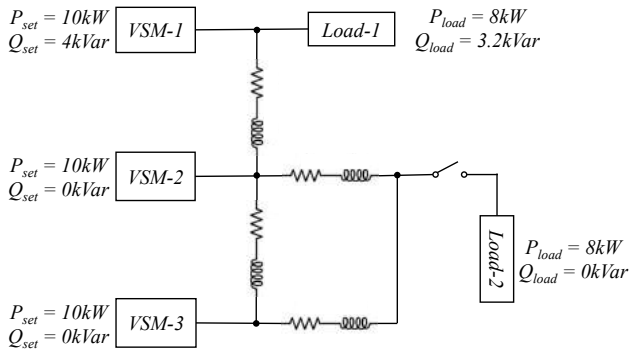


Fig. 5. One phase of the microgrid in our simulations

Each inverter is designed to supply a nominal active power $P_n = 10\text{kW}$ and reactive power $Q_n = 4\text{kVar}$ at the grid frequency $\omega_g = 100\pi$ rad/sec (50Hz) and the line voltage $V = 230\sqrt{3}$ Volts. Following the empirical guidelines from Natarajan and Weiss (2018), the parameters of the LC filter are: $R_s = 0.1\Omega$, $L_s = 2.2\text{mH}$, $C_s = 10\mu\text{F}$. The transmission line segments are identical, with parameters $R = 1.1\text{m}\Omega$ and $L = 0.1\text{H}$. When using the older approach, the parameter n from Fig. 2 was 25.

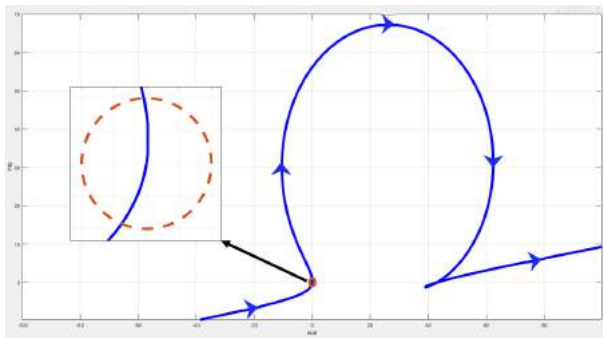


Fig. 6. Nyquist plot of the loop gain with the plant (13) and the proposed current controller as shown in Fig. 3. The plot in the box is the zoomed in region of the Nyquist plot shown by a black arrow. The dashed red line is the unit circle in \mathbb{C} .

In the design of the current controller, following the design outlined in Section 3, we choose $\omega_b = 1000\text{rad/sec}$, $K_p = (4.3 - 0.6912j)\Omega$, $K_i = 2200\Omega\cdot\text{sec}$. We have $z = (45.45 + 314.16j)\text{sec}^{-1}$. The resulting Nyquist plot of the current loop gain (the loop gain corresponding to Fig. 3) is shown in Figure 6. This is a very unusual, non-symmetric Nyquist plot, because two coefficients in the loop gain are not real. The Matlab computation shows that the system has gain margin ∞ , phase margin 67.4° and cross-over frequency 1822 rad/sec. The reference currents were generated as explained in Section 3, using a virtual output impedance composed of $R_{virt} = 2\Omega$ and $L_{virt} = 50\text{mH}$.

The set points for inverters and the loads are chosen as shown in Fig. 5. VSM-1 starts working at $0[\text{sec}]$ and behaves as a (pseudo) grid to the rest of the microgrid system. Load-1 starts receiving the required power from this grid. VSM-2 starts synchronizing with the grid at $20[\text{sec}]$. It connects to the grid and starts delivering the power once synchronization process is done. At $40[\text{sec}]$, Load-2 is connected to the grid. VSM-3 starts to synchronize with the grid at $60[\text{sec}]$ and starts delivering power to the

loads once synchronized. We have simulated the effect of the voltage measurement noise by adding low-pass filtered independent discrete white noise signals to each of the 9 voltage measurements present in the microgrid of Fig. 5 (at the sampling frequency of 10 kHz). We have taken the bandwidth of each of the 9 low-pass filters to be 300 Hz and we have adjusted the standard deviation of the white noise such that the standard deviation of the filtered noise signal (the voltage measurement error) is 4 Volt. In addition, we have added a pure sine wave of amplitude 4 Volt and frequency 150 Hz to the voltage measurement of phase a in VSM-1. Figure 7 shows the current in phase 1 of VSM-1 at a time segment when two synchronverters are working together (with one load). We see that with the older algorithm, the amplitude of the current (the blue plot) is not steady, and also the THD is much higher (but this is hard to see with the naked eye in this figure).

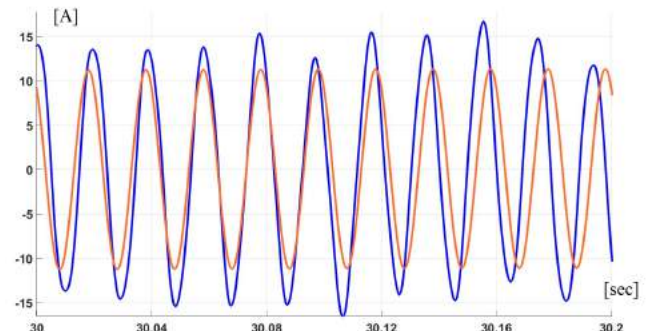


Fig. 7. A portion of the plot of the current in phase 1 of VSM1 when all the synchronverters in the microgrid use the older algorithm (blue) and when they use the new algorithm proposed here (red). We see that the new algorithm is more stable.

We can see in Fig. 8 that even with errors in the voltage measurements the system with the new approach behaves very well. We can notice that the power sharing between the 3 inverters is done more equally in the new approach as compared to the older approach. We can also notice in Fig. 8 that the frequency of the inverters is very close to 50Hz most of the time in current control approach with help of secondary control (which will be elaborated in the journal version of this paper). The loads receive the desired power, as can be seen in Fig. 9. With the older approach, the power is much more noisy, and VSM-1 is the most noisy because it receives a sinusoidal measurement noise in addition to the filtered white noise, as explained before.

5. CONCLUSIONS

We have proposed a modification of the synchronverter control algorithm, to improve the robustness to the inevitable voltage and current measurement errors during operation. The improved control scheme has been verified by simulations and hardware in the loop experiments. The simulation results clearly show that the proposed current loop control significantly improves stability of the synchronverter during operation.

REFERENCES

Alipoor, J., Miura, Y. and Ise T. (2013). Distributed generation grid integration using virtual synchronous

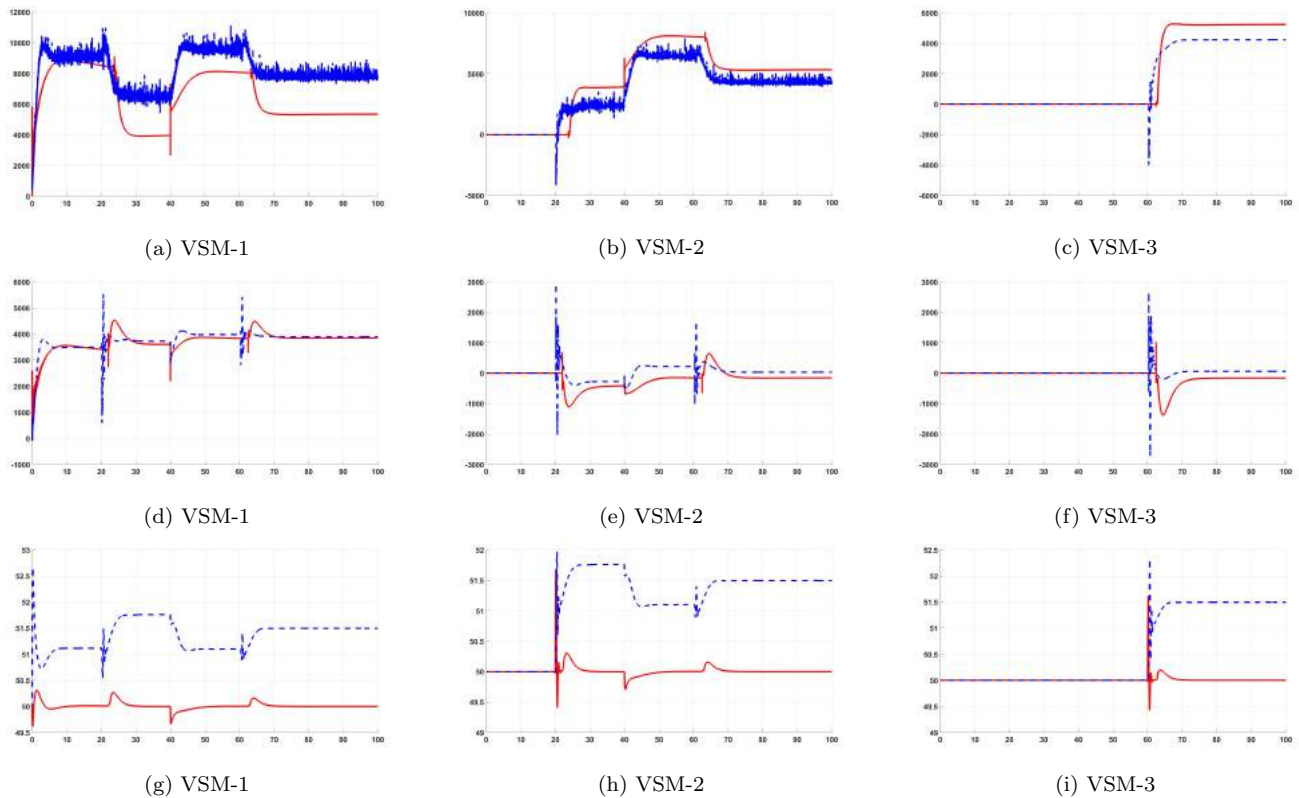


Fig. 8. 8a, 8b, 8c represent the active power delivered by the inverters. 8d, 8e, 8f represent the reactive power delivered by the inverters. 8g, 8h, 8i represent the frequency of the inverters. Here, the dashed (blue) curve represents the older synchronverter approach and the solid (red) curve represents the proposed newer approach with current control.

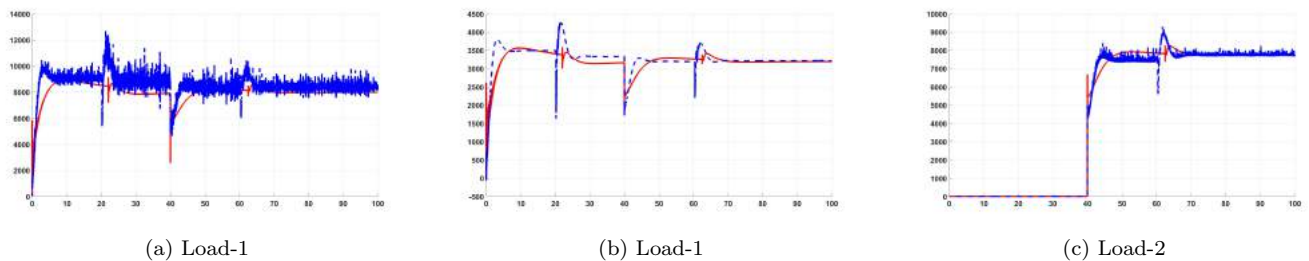


Fig. 9. 9a, 9b represent the active power and reactive power on Load-1 respectively. 9c represents the active power on Load-2. We follow the same conventions as Fig. 8 for dashed (blue) and solid (red) curves.

generator with adaptive virtual inertia. *Proc. IEEE Energy Conversion Congress and Exposition (ECCE)*, Denver, CO, pp. 4546-4552.

Aouini, R., Marinescu, B., Kilani, K.B. and Elleuch M. (2015). Synchronverter-based emulation and control of HVDC transmission. *IEEE Trans. Power Systems*, vol. 31, pp. 278-286.

Arghir, C., Jouini, T. and Dörfler, F. (2018). Grid-forming control for power converters based on matching of synchronous machines. *Automatica*, 95, 273-282.

Beck, H.P. and Hesse, R. (2007). Virtual synchronous machine. *Proc. 9th Int. Conf. on Electrical Power Quality and Utilisation (EPQU)*, 1-6.

Brown, E. (2015). A Study of the Use of Synchronverters for Grid Stabilization Using Simulations in SimPower. *MSc thesis*, Tel Aviv University.

Cvetkovic, I., Boroyevich, D., Burgos, R., Li, C., and Mattavelli, P. (2015). Modeling and control of grid-connected voltage-source converters emulating isotropic and anisotropic synchronous machines. *Proc. 16th IEEE Workshop on Control and Modeling for Power Electronics (COMPEL)*, Vancouver, Canada.

Dong, S., Chi, Y.N. and Li, Y. (2016). Active voltage feedback control for hybrid multi-terminal HVDC system adopting improved synchronverters. *IEEE Trans. on Power Delivery*, vol. 31, pp. 445-455.

Driesen, J. and Visscher, K. (2008). Virtual synchronous generators. *IEEE Power and Energy Soc. General Meeting - Conversion and Delivery of Electrical Energy in the 21st Century*, Pittsburg, PA, pp. 1-3.

Grainger, J.J. and Stevenson, W.D. (1994). *Power Systems Analysis* McGraw-Hill, New York.

Konstantopoulos, G., Zhong, Q.C., Ren, B. and Krstic, M. (2015). Bounded integral control for regulating input-to-state stable non-linear systems. *Proc. American Control Conference (ACC 2015)*, Chicago, IL, USA, pp. 4024-4029.

- Kundur, P. (1994). *Power System Stability and Control*. McGraw-Hill, New York.
- Kustanovich, Z., Shivratri, S. and Weiss, G. (2020a). The sensitivity of synchronverters with respect to measurement errors. *in preparation*.
- Kustanovich, Z., Shivratri, S. and Weiss, G. (2020b). Virtual synchronous machines with fast current loop and secondary control. *in preparation*.
- Lifshitz, D. and Weiss, G. (2015). Optimal control of a capacitor-type energy storage system. *IEEE Trans. on Automatic Control*, vol. 60, pp. 216-220.
- Lorenzetti, P., Weiss, G. and Natarajan, V. (2019). Integral control of stable nonlinear systems based on singular perturbations. *submitted*.
- Mandel, Y. and Weiss, G. (2015). Adaptive internal model based suppression of torque ripple in brushless DC motor drives. *Systems Science & Control Engineering*, vol. 5, pp. 162-176.
- Mo, O., D'Arco, S. and Suul, J.A. (2017). Evaluation of virtual synchronous machines with dynamic or quasi-stationary machine models. *IEEE Trans. Ind. Electronics*, vol. 64, pp. 5952-5962.
- Natarajan, V. and Weiss, G. (2017). Synchronverters with better stability due to virtual inductors, virtual capacitors and anti-windup. *IEEE Trans. on Industrial Electronics*, vol. 64, pp. 5994-6004.
- Natarajan, V. and Weiss, G. (2018). Almost global asymptotic stability of a grid-connected synchronous generator. *Math. of Control, Signals and Systems*, vol. 30.
- Roldan-Perez, J., Rodriguez-Cabero, A. and Prodanovic, M. (2018). Parallel current-controlled synchronverters for voltage and frequency regulation in weak grids. *Proc. of 9th Int. IET Conference on Power Electronics, Machines and Drives (PEMD 2018)*, Liverpool, UK.
- Sauer, P.W. and Pai, M.A. (1997). *Power Systems Dynamics and Stability*. Stipes Publishing, Champaign, IL, USA.
- Tayyebi, A., Gross, D., Anta, A., Kupzog, F. and Dörfler, F. (2020). Frequency stability of synchronous machines and grid-forming power converters. *IEEE Journal of Emerging and Selected Topics in Power Electronics*.
- Timbus, A., Liserre, M., Teodorescu, R., Rodriguez, P. and Blaabjerg, F. (2009). Evaluation of current controllers for distributed power generation systems. *IEEE Transactions on Power Electronics*, 24(3), 654-664.
- Wang, X., Li, Y.W., Blaabjerg, F. and Loh, P.C. (2015). Virtual-impedance-based control for voltage-source and current-source converters. *IEEE Trans. Power Electronics*, vol. 30, pp. 7019-7037.
- Weiss, G., Dörfler, F. and Levron, Y. (2019). A stability theorem for networks containing synchronous generators. *Systems & Control Letters*, vol. 134.
- Wu, H., Ruan, X., Yang, D., Chen, X., Zhao, W., Lv, Z. and Zhong, Q.C. (2016). Small-signal modeling and parameters design of virtual synchronous generators. *IEEE Trans. Industrial Electronics*, vol. 63, pp. 4292-4303.
- Yu, M., Dysko, A., Booth, C., Roscoe, A., Zhu, J. and Urdal, H. (2015). Investigations of the constraints relating to penetration of non-synchronous generation in future power systems. *Protection, Automation and Control (PAC) World Conf.*, Glasgow, UK.
- Zhong, Q.C. and Hornik, T. (2013). *Control of Power Inverters in Renewable Energy and Smart Grid Integration*. Wiley, Chichester, UK.
- Zhong, Q.C., Konstantopoulos, G.C., Ren, B. and Krstic, M. (2018). Improved synchronverters with bounded frequency and voltage for smart grid integration. *IEEE Trans. Smart Grid*, vol. 9, pp. 786-796.
- Zhong, Q.C., Nguyen, P.L., Ma, Z. and Sheng, W. (2014). Self-synchronized Synchronverters: Inverters without a dedicated synchronization unit. *IEEE Trans. Power Electronics*, vol. 29, pp. 617-630.
- Zhong, Q.C. and Weiss, G. (2009). Static synchronous generators for distributed generation and renewable energy. *Proc. IEEE PES Power Systems Conf. & Exhibition (PSC)*, Washington, USA.
- Zhong, Q.C. and Weiss, G. (2011). Synchronverters: Inverters that mimic synchronous generators. *IEEE Trans. Industr. Electronics* 58, vol. 58, pp. 1259-1267.